

Synthesis of Metal Oxide Nanoparticles by Rapid, High-Temperature 3D Microwave Heating

Geng Zhong, Shaomao Xu, Chaoji Chen, Dylan Jacob Kline, Michael Giroux, Yong Pei, Miaolun Jiao, Dapeng Liu, Ruiyu Mi, Hua Xie, Bao Yang, Chao Wang, Michael R. Zachariah, and Liangbing Hu*

Microwave-assisted fabrication has propelled the recent synthesis and processing approaches of various nanomaterials. However, in most previous studies, the synthesis temperature is limited to below 1100 K, which restricts its application. Here, a rapid, in situ 3D heating method to manufacture well-dispersed metal oxide nanoparticles on a 3D carbonized wood (denoted as C-wood) host using microwaves as the driving power is reported. The moderate electronic conductivity of C-wood contributes to the local Joule heating and the good thermal conductivity guarantees the rapid 3D heating of the overall material. The temperature of the C-wood increases from room temperature to ≈ 2200 K in 4 s (≈ 550 K s⁻¹), stabilizing to 1400 K, and then cooling back down to room temperature within 2 s. The preloaded precursor salts rapidly decompose and form ultrafine (≈ 11 nm) metal oxide nanoparticles on the surface of the C-wood during the rapid quenching. The process takes place in air, which helps prevent the metal oxides from being reduced by the carbon. The 3D heating method offers an effective route to the rapid and scalable synthesis of metal oxide nanoparticles.

1. Introduction

Carbon-supported metal oxide nanoparticles have been widely used in water treatment,^[1] photovoltaic cells,^[2–4] supercapacitors,^[5–7] and alkali-ion batteries.^[8,9] In such applications, the

G. Zhong, Dr. S. Xu, Dr. C. Chen, M. Jiao, D. Liu, R. Mi, H. Xie, Prof. L. Hu
Department of Materials Science and Engineering
University of Maryland
College Park, MD 20742, USA
E-mail: binghu@umd.edu

D. J. Kline, Prof. M. R. Zachariah
Department of Chemistry
University of Maryland
College Park, MD 20742, USA

M. Giroux, Prof. C. Wang
Department of Chemical and Biomolecular Engineering
Johns Hopkins University
Baltimore, MD 21218, USA

Y. Pei, Prof. B. Yang
Department of Mechanical Engineering
University of Maryland
College Park, MD 20742, USA

 The ORCID identification number(s) for the author(s) of this article can be found under <https://doi.org/10.1002/adfm.201904282>.

DOI: 10.1002/adfm.201904282

carbon substrate not only acts as a conductive host but also prevents the nanoparticles from aggregating to optimize their functionality. High-temperature processing is typically used to synthesize metal oxide nanoparticles decorated on carbon. The uniform and high temperature enables the sufficiently fast reaction kinetics which is critical to the formation of ultrafine nanoparticles. However, in traditional heating techniques (e.g., tube furnace heating), there is a temperature gradient from the surface to the interior of the substrate.^[10] Furthermore, the heat is transferred by conduction, radiation, and convection, which are often inefficient, nonuniform, and time consuming for heating bulk materials. Moreover, extended high-temperature processing in an inert environment can cause reduction of the metal oxides by the carbon sub-

strate. As a result of these limitations, nontraditional heating techniques have been developed, including laser heating, which provides rapid and localized heating for the synthesis of nanoparticles.^[11,12] However, the laser heating method can only heat a thin layer of the surface of the sample and is highly dependent on the laser absorption capacity of the target material, which is difficult to control.^[13,14]

Microwave-assisted heating has been widely used for decades in the synthesis and processing of functional materials as it drastically reduces the reaction time and dramatically improves the heating efficiency.^[15–17] Recently, microwave heating has been applied to the synthesis of advanced nanomaterials, including high-quality graphene,^[18] graphene-supported catalysts,^[19] carbon nanotube (CNT)/MXene composites,^[20] and ceramic electrolyte.^[21] However, these methods failed to reach a high temperature (>1100 K), thus limiting the application of microwave heating.

Wood features a natural 3D channel structure along the growth direction for the transport of water, ions, and other substances.^[22] This unique structure has enabled various emerging applications, such as energy storage,^[23,24] thermal management,^[25] and water extraction.^[26,27] Taking advantage of this natural and abundantly available resource, in this work we demonstrate a microwave-triggered 3D heating method in air for the rapid, in situ synthesis of metal oxide nanoparticles

using carbonized wood (C-wood) as a 3D heating substrate. We show that suitable electronic conductivity ($\approx 1.6 \text{ S cm}^{-1}$), good thermal conductivity, and unique 3D channeled structure play critical roles in the microwave ignition of the C-wood. During microwave treatment, the abundant, thin carbon walls of C-wood effectively absorb microwave radiation without obvious transmission or reflection. The moderate conductivity of the C-wood transfers the electromagnetic energy to thermal energy through Joule heating, leading to a rapid temperature increase, from room temperature to $\approx 2200 \text{ K}$ in 4 s. In this manner, we are able to achieve an average and maximum instantaneous heating rate of ≈ 550 and $\approx 272\,000 \text{ K s}^{-1}$, respectively, which are orders of magnitude faster than that achieved in conventional furnace chamber heating ($< 1 \text{ K s}^{-1}$). The high temperatures achieved enable fast precursor salt decomposition, and the rapid temperature quenching ($< 2 \text{ s}$) causes metal oxide nanoparticles to recrystallize on the surface. Furthermore, the short reaction time prevents the ablation of the carbon host and the air condition keeps the metal oxides from being reduced by the carbon. The 3D heating method can reach and keep a temperature as high as $\approx 1400 \text{ K}$, which enables the decomposition of

most nitrate salts. Thus, a range of metal oxide nanoparticles can be readily fabricated on C-wood using this universal and rapid 3D heating method.

2. Results and Discussion

Figure 1a demonstrates how the rapid 3D heating was triggered in a domestic microwave oven in an air environment. Specifically, a 1000 W microwave power lasting for 9 s ($\approx 5 \text{ s}$ induction period and $\approx 4 \text{ s}$ reaction period) was applied to the C-wood substrate ($30.0 \text{ mm} \times 12.0 \text{ mm} \times 3.5 \text{ mm}$) to achieve rapid heating. During this process, the temperature of the C-wood can be ramped to as high as 1400 K , accompanied by a bright light due to black-body radiation (Figure 1b). We hypothesized that this instantaneous 3D heating could be used as an effective strategy to synthesize metal oxide nanoparticles decorating the substrate by loading metal salt precursors within the C-wood channels prior to microwaving (Figure 1c). Thus the precursors, which were hundreds of nanometers in size, were decomposed into $\approx 11 \text{ nm}$ metal oxide nanoparticles attached to

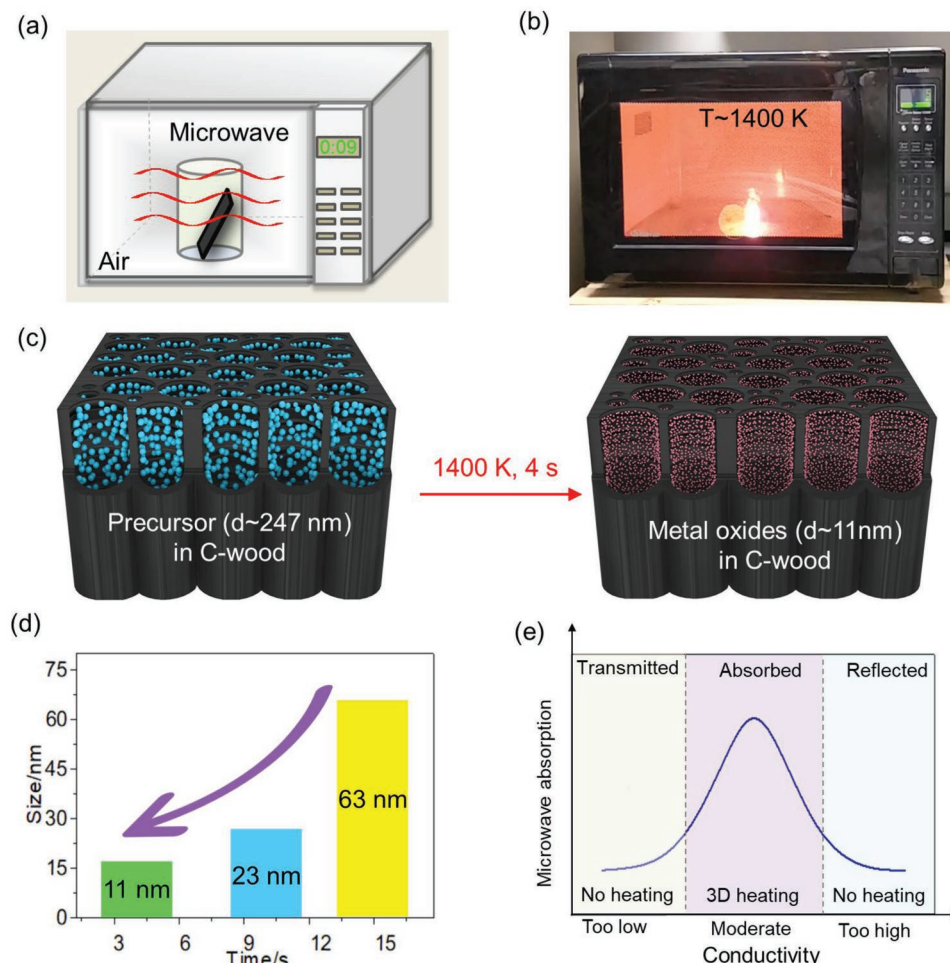


Figure 1. a) Schematic of the microwave heating setup. b) Image of the heating process taking place and the resulting light emitted from the material. c) Schematic of metal oxide nanoparticles fabricated within the C-wood substrate by the 3D heating treatment at $\approx 1400 \text{ K}$ for 4 s. d) Average nanoparticle size as a function of the heating duration. e) The effect of electronic conductivity on the microwave coupling and the resulting heating effect of C-wood.

the wood cell walls (Figure 1c). As we increased the reaction time from 4 to 10 and 15 s, we found that the average size of nanoparticles increased from ≈ 11 to ≈ 23 and ≈ 63 nm, respectively (Figure 1d). Therefore, it is easy to control the size of the nanoparticle by simply adjusting the radiation time. We note that the electronic conductivity (σ) of C-wood is a vital factor in the microwave coupling and 3D heating effect. Only C-wood with moderate σ can absorb the microwave radiation effectively and give rise to the 3D heating, while insulating and highly conductive C-wood are either microwave transparent or reflective, and as a result demonstrate no high-temperature 3D heating (Figure 1e).

As a demonstration of the effectiveness of this method, we applied $\text{Co}(\text{NO}_3)_2$ to the C-wood (C-wood/ $\text{Co}(\text{NO}_3)_2$) and microwaved it for ≈ 4 s heating to produce well-dispersed cobalt oxide (CoO_x) nanoparticles in the C-wood (C-wood/ CoO_x). The C-wood used as a 3D microwave susceptor was prepared by directly carbonizing the natural wood at 973 K. Then, we dipped the C-wood into the ethanol solution of $\text{Co}(\text{NO}_3)_2$ and dried the material in air to form the C-wood/ $\text{Co}(\text{NO}_3)_2$ precursor for 3D heating, which we triggered by microwave radiation. Figure 2a,b shows photos of the C-wood/ $\text{Co}(\text{NO}_3)_2$ before and after 3D heating, displaying no obvious difference. Similarly, the Raman spectrum of the material also remains unchanged (Figure S1, Supporting Information), suggesting no morphological or structural damage was induced to the C-wood by the instant high temperature. Figure 2c,d depicts the scanning electron microscopy (SEM) images of the C-wood/ $\text{Co}(\text{NO}_3)_2$ and C-wood/ CoO_x materials. Before 3D heating, the hierarchical and aligned channels along the tree-growth direction can be clearly seen, which originate from the vessels in the natural wood (Figure S2, Supporting Information).^[28] A corresponding high-resolution SEM image shows that the $\text{Co}(\text{NO}_3)_2$ precursor with irregular shapes are distributed on the cell walls. By measuring the two farthest points on the particle, we estimated that the sizes of the particles are hundreds of nanometers. After 4 s of 3D heating, although the temperature reached is high, the duration of the heating is so short that the channeled structure of the C-wood remains unchanged (Figure 2d). However the high temperature leads to the rapid decomposition of the $\text{Co}(\text{NO}_3)_2$ precursor and the formation of CoO_x nanoparticles inside the C-wood channels (Figure 2f). The rapid heating and cooling processes effectively limit the aggregation of the nanoparticles, enabling the small size (≈ 11 nm) and uniform distribution of CoO_x nanoparticles throughout the bulk C-wood substrate.

Although carbon materials are not exactly a black-body source, their brightness is above the black level and within the error threshold that can be effectively adopted to report mean and median temperature.^[29] We performed color ratio pyrometry to study the temperature evolution during the microwave heating using high-speed camera to capture the sample's color change. The images are computer-processed to capture the raw color of each pixel and enabling spatial and time resolved ratio pyrometer to get temperature. Figure 2g shows a plot of the sample light emission intensity versus time over the initial 200 ms of lighting (starting at ≈ 5 s after microwave is turned on). Visible emission is observed at the ≈ 25 th ms, then increased rapidly until ≈ 70 ms, and subsequently dimmed until

the microwave stopped. The photos of this heating process are shown in Figure S3 in the Supporting Information, which is in good accordance with the light intensity spectrum of Figure 2g. According to the black-body fitting, the temperature rises rapidly from below 1200 to 2200 K within less than 50 ms and falls sharply to 1400 K within 25 ms after the temperature peak (Figure 2h). Thereafter, the temperature remains uniform and stable at ≈ 1400 K, which agrees well with the temperature profiles calculated from high speed pyrometry frames (Figure 2i). This temperature induced by this process is high enough to drive the decomposition of $\text{Co}(\text{NO}_3)_2$ (decomposition temperature ≈ 350 K). Note that even using a reduced microwave power, a similar temperature (with temperature difference of <30 K) can still be achieved, indicating that our strategy can be more energy efficient (Figure S4, Supporting Information). This is further evidenced by the similar sizes and shapes of the particles synthesized by different microwave powers (Figure S5, Supporting Information).

To further demonstrate the uniformity of this 3D heating method, a larger C-wood/ $\text{Co}(\text{NO}_3)_2$ (30 mm \times 15 mm \times 7 mm) sample was treated with this 3D heating method for 6 s. Figure 3a is the SEM image of the resulting C-wood/ CoO_x , which shows that the open channels in the C-wood are well preserved after 3D heating. We examined three different regions along the thickness direction marked in the SEM image by transmission electron microscopy (TEM) to show the distribution of CoO_x nanoparticles throughout the C-wood substrate (Figure 3b–d). Even with the larger C-wood size, we observed a similar distribution of CoO_x nanoparticles throughout the three selected regions, demonstrating the good uniformity of this 3D heating method. We calculated from the TEM images that the average diameter of the CoO_x nanoparticles in this material was ≈ 12 nm, similar to that of the smaller C-wood block, suggesting the potential scalability of this 3D heating method. The X-ray diffraction (XRD) patterns of the C-wood/ CoO_x show that there are two kinds of oxides present, CoO and Co_3O_4 (Figure 3e). The energy dispersive X-ray (EDX) elemental maps illustrate the elemental distribution of cobalt and oxygen which coincides with that of the nanoparticles on the C-wood, confirming the chemical composition of the synthesized nanoparticles (Figure 3f–h).

Similar to our previous report, we note that the duration of high temperature has great influence on the structure and size of the resultant particles.^[30,31] As shown in Figure S6a–d in the Supporting Information, when the heating time is less than 2 s, there are many irregularly shaped fragments distributed on the surface of the wood channels. At this limited heating time, we believe that the reaction stopped before the newly generated CoO_x could fully form the targeted nanoparticle structures. However, we can obtain uniform nanoparticles when the heating time is longer than 4 s (Figure S6e–h, Supporting Information). The size of the nanoparticles increases with the heating time, the average diameter of which are ≈ 11 nm for 4 s, ≈ 23 nm for 10 s, and ≈ 63 nm for 15 s heating, respectively, demonstrating the temporal confinement of the heating time on the synthesis of fine nanoparticles. Note that the metal oxide nanoparticles decorating the carbon matrix can be used in many fields, such as solar cells,^[4] electrocatalysis,^[32] and lithium-ion batteries.^[8] The C-wood matrix with channeled

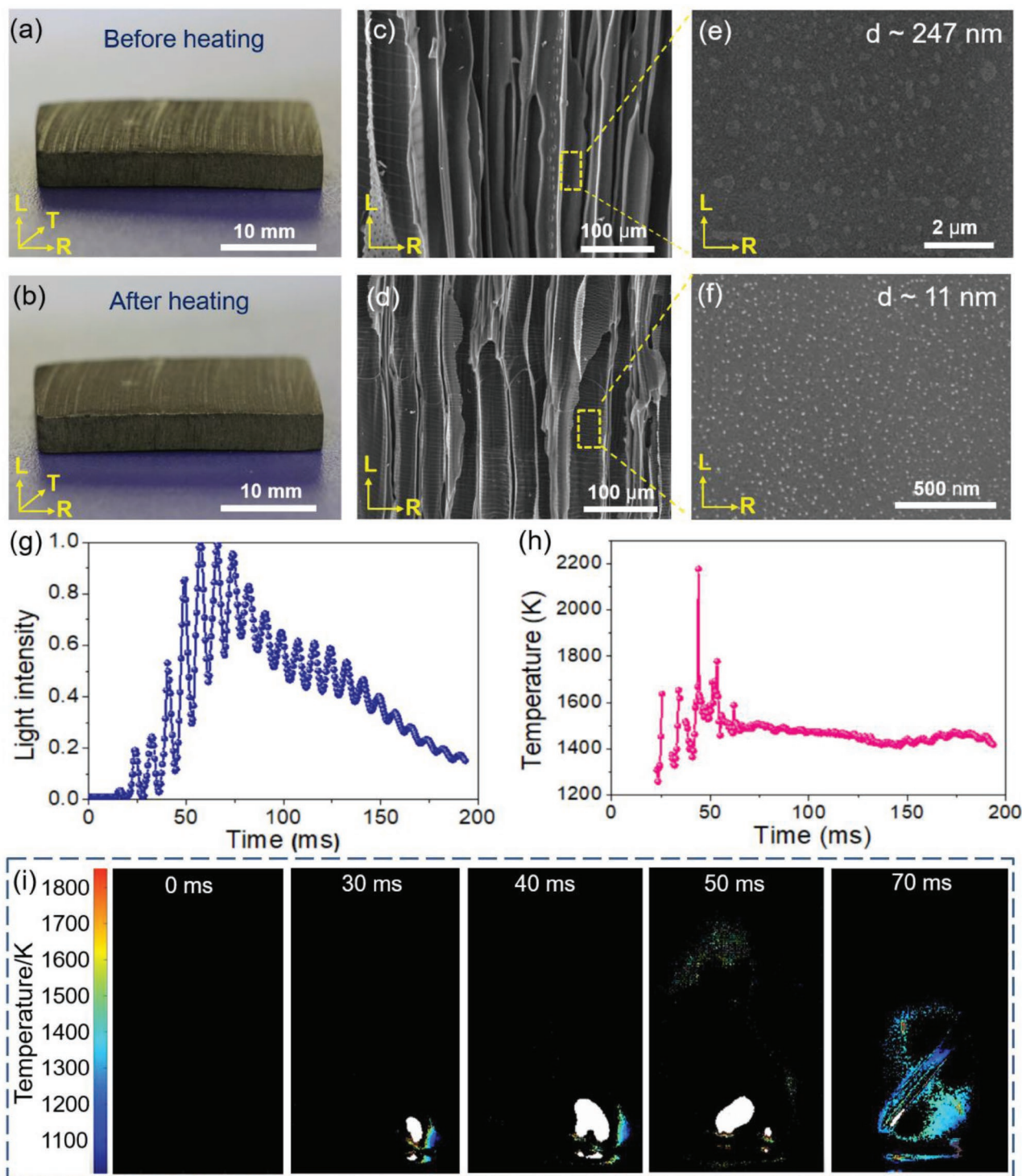


Figure 2. Characterization of the rapid 3D heating method. Photos of the a) C-wood/ $\text{Co}(\text{NO}_3)_2$ starting material before and b) the resulting C-wood/ CoO_x after the microwave heating process. SEM images of the c) C-wood/ $\text{Co}(\text{NO}_3)_2$ and d) C-wood/ CoO_x materials, and e,f) the corresponding high-resolution images, indicating the successful generation of nanoparticles on the C-wood channels after microwave heating. g) Emitted light intensity of the initial 200 ms of 3D heating at 1000 W. h) The temporal evolution of the temperature estimated from the light intensity according to the black-body theory. i) Temperature profiles of the initial 70 ms lighting calculated from high-speed pyrometry frames.

structure provides a conductive support for CoO_x nanoparticles and could enable gases/solutions to flow throughout the structure for catalysis.

Unlike in polar materials, where the dipoles rotate with the change of the electric field to cause friction and heating, C-wood has few rotating dipoles to generate heat.^[33,34] The

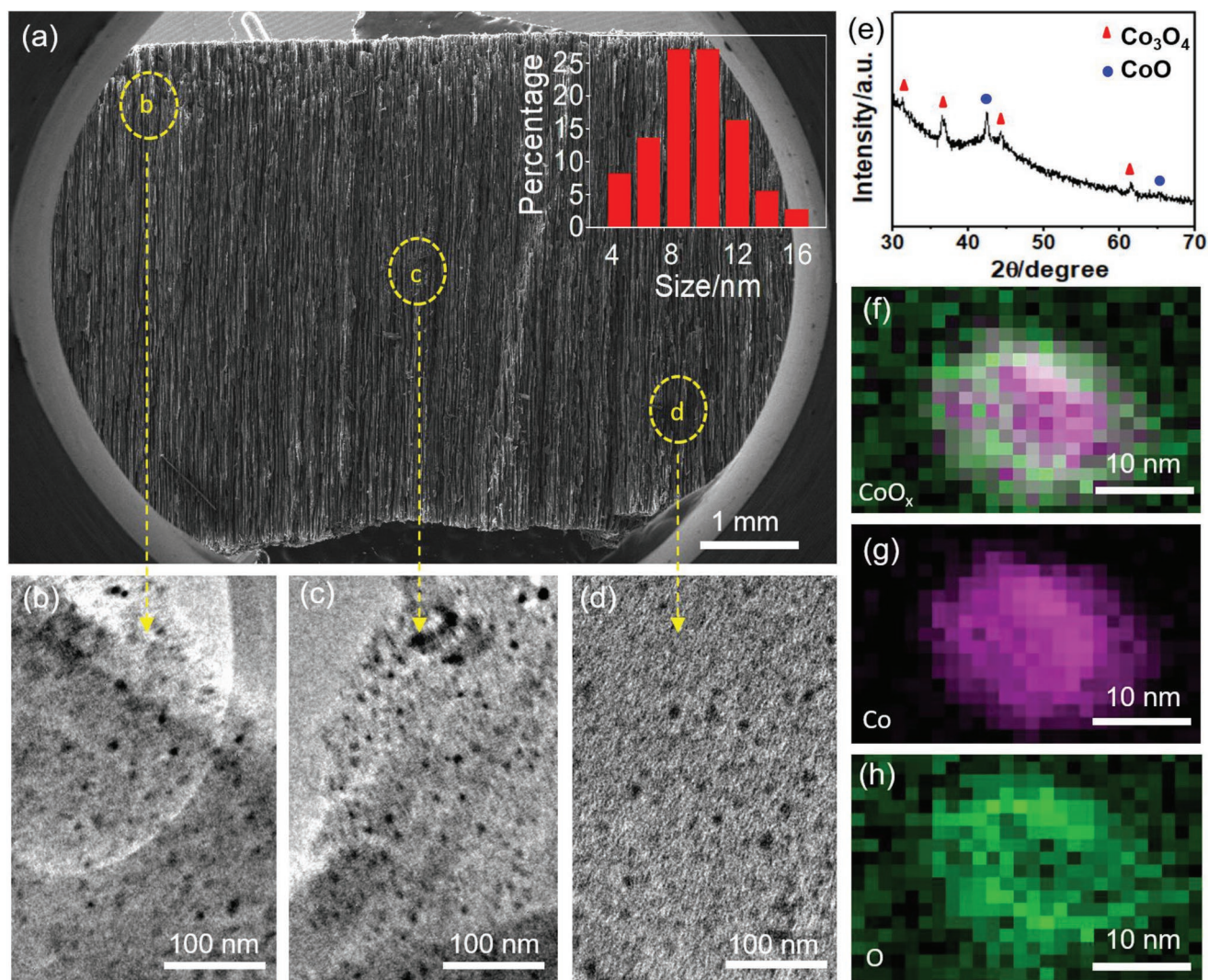


Figure 3. Microstructure of the C-wood/CoO_x made by 6 s of the rapid 3D heating. a) SEM image of the C-wood/CoO_x composite, showing the well-preserved vertically aligned channels after microwave heating treatment. b–d) TEM images of the samples selected from the three corresponding regions in (a). e) XRD patterns of C-wood/CoO_x, suggesting that the nanoparticles consist of CoO and Co₃O₄. f) The combined and individual g) Co and h) O EDX maps of a nanoparticle found in the C-wood/CoO_x, fabricated by 6 s of heating.

possible mechanism behind this heating process may be microwave-induced Joule heating. Specifically, microwaves, featuring an oscillating magnetic field, can trigger an induced current (I_i) in C-wood with suitable conductivity. The direction of I_i will change with that of the oscillating magnetic field.^[35] Therefore, the microwave energy transfers to heat through Joule heating, leading to a rapid and uniform 3D heating. It has been shown that a moderate electronic conductivity (σ) is of great importance for the absorption of microwaves and fast heating.^[36,37] Figure 4a–c is the schematics that show different heating effects of C-wood that features different conductivities. As shown in Figure 4a, when the σ is too low, the C-wood is transparent to microwaves and will cause no high-temperature heating. Conversely, when the σ is too high, the C-wood will reflect most of microwaves, leading to the failure of high-temperature heating (Figure 4c). In both cases, the temperature of C-wood is not high enough to emit bright light. Only when the

σ is in a moderate range can high-temperature 3D heating be induced (Figure 4c).

To further study the microwave heating mechanism, we examined the microwave absorption performance and thermal conductivity of C-wood featuring different σ . The C-wood with different σ are obtained by carbonizing the natural wood in Ar at different temperatures. As shown in Figure 4d, σ increases with the carbonization temperature, in which we found that temperatures of 873, 973, and 1273 K resulted in conductivities of 4.8×10^{-5} , 1.6, and 9.8 S cm^{-1} , respectively. This difference in σ causes dramatic changes in the microwave absorption performance. When microwave radiation is incident on an object, the electromagnetic energy dissipates through three ways, including transmission, absorption, and reflection.^[38] The corresponding coefficients can be viewed as the proportion of dissipated energy to incident microwave energy. As shown in Figure 4e, the microwave absorption coefficient of the C-wood

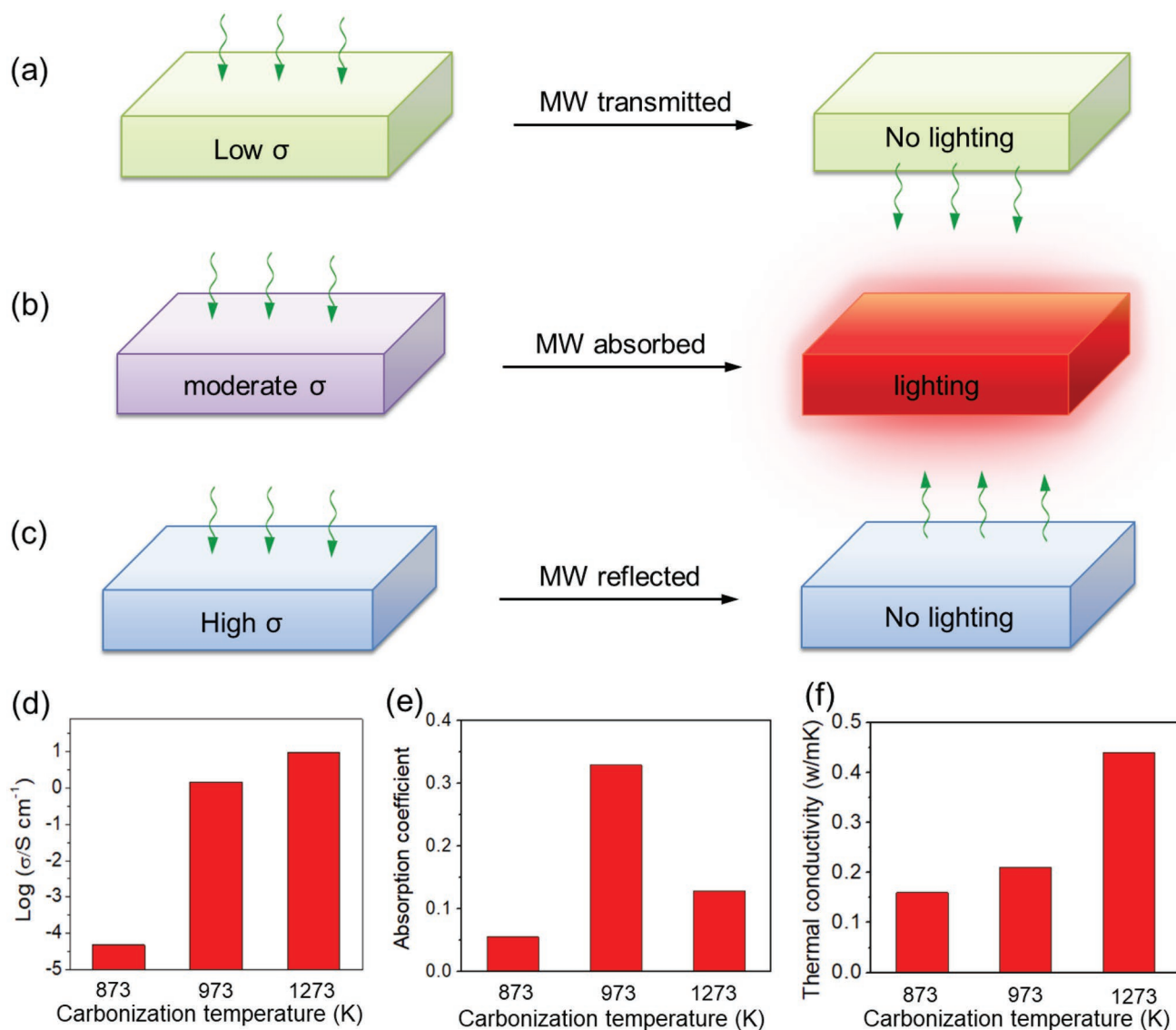


Figure 4. Mechanism of the 3D heating method. a–c) Schematics of microwave coupling behaviors and the heating effects of C-wood with different electronic conductivities. d) Electronic conductivities of C-wood carbonized at different temperatures. e) Microwave absorption performance of C-wood with different electronic conductivities made at different temperatures. f) Thermal conductivities of C-wood carbonized at different temperatures.

treated at 973 K is 0.33, which is much higher than the insulating sample treated at 873 K (0.05) and the highly conductive C-wood carbonized at 1273 K (0.13), enabling it to couple large amounts of electromagnetic energy. This energy is then rapidly converted to thermal energy via a Joule heating mechanism, leading to high-temperature 3D heating. The detailed plots of coefficients (Figure S7, Supporting Information) show that $\approx 80\%$ of microwave radiation is either transmitted or reflected in the insulated or highly conductive C-wood, leading to the lack of high-temperature heating. Note that the composition of the C-wood has a great influence on electronic conductivity, thus can significantly affect the microwave absorption capability. As the carbonization temperature increases, the amounts of functional groups and defects decrease (Figure S8a,b, Supporting Information), leading to a higher electronic conductivity (Figure S7a,b, Supporting Information). Therefore, combined

with the previous analysis, the suitable amounts of functional groups and defects are important for the moderate electronic conductivity of C-wood and the corresponding high microwave absorption (Figure 4a–e).

In addition to the microwave absorption capability, the thermal conductivity is also important to the 3D volumetric heating. Figure 4f shows the thermal conductivities of the different C-wood samples. The thermal conductivity of wood treated at 973 K is between that of the 873 and 1273 K samples, which is able to timely transmit the induced heat throughout the object, leading to rapid 3D volumetric heating.

The minimal size of the C-wood is another important factor for high microwave absorption and high-temperature heating. We accidentally observed that the cracked piece of C-wood was not an effective microwave absorbent which was unable to trigger high-temperature heating compared to its unbroken

counterpart (Figure S9, Supporting Information). To understand the reason of this sharp contrast, a series of microwave heating processes were carried out based on C-wood samples (carbonized at 973 K) with size of 0.3 cm (height) \times 0.4 cm (width) \times 0.5, 1.0, 2.0, 3.0, and 4.0 cm (length). No light emission was observed when the length is below 2.0 cm, indicating that the temperature is much lower than 1000 K. On the other hand, when the length is above 2.0 cm, all the samples showed strong light emission, signifying that the high temperature was achieved. Moreover, the temperature evolution shows a similar temperature of \approx 1380 K with a very small difference less than 50 K (Figure S10a,b, Supporting Information). These results demonstrate that a sample with suitable size and electronic conductivity is critical for microwave absorption, ignition (via Joule heating), and subsequent 3D bulk heating.

Since the thermal decomposition of metal salts is a universal reaction mechanism, this synthesis method should not be exclusive to CoO_x nanoparticles. To demonstrate the universality of our technique, we also synthesized NiO and Fe_3O_4 nanoparticles via C-wood substrates and microwave heating. Figure 5a,e is the SEM images of the C-wood/NiO and C-wood/ Fe_3O_4 samples, respectively, which show that the resulting nanoparticles are uniformly distributed in the C-wood substrate. The TEM

images and size distributions of C-wood/NiO (Figure 5b) and C-wood/ Fe_3O_4 (Figure 5f) show that the average sizes of these nanoparticles are \approx 29 and 18 nm, respectively. Elemental mapping of the metal and oxygen contents can verify the qualitative distribution of these materials (Figure 5c,d,g,h). Furthermore, the XRD patterns (Figure 5i,j) confirm the crystal structures of the synthesized nanoparticles, which match the standard curves of NiO and Fe_3O_4 . Our 3D heating method can raise the temperature to as high as 1400 K, which well exceeds the decomposition temperature of most metal nitrates, including cobalt, nickel, and iron (Figure 5k). Therefore, a range of metal oxide nanoparticles can be successfully synthesized via this rapid and efficient method.

3. Conclusion

In summary, we report a rapid microwave bulk heating method for the in situ synthesis of ultrafine metal oxide nanoparticles on a channel-structured C-wood substrate. Compared with conventional heating methods, this 3D heating technique is simpler, faster, and more efficient. The temperature of the C-wood can reach up to 2200 K in 4 s and remains stable at 1400 K,

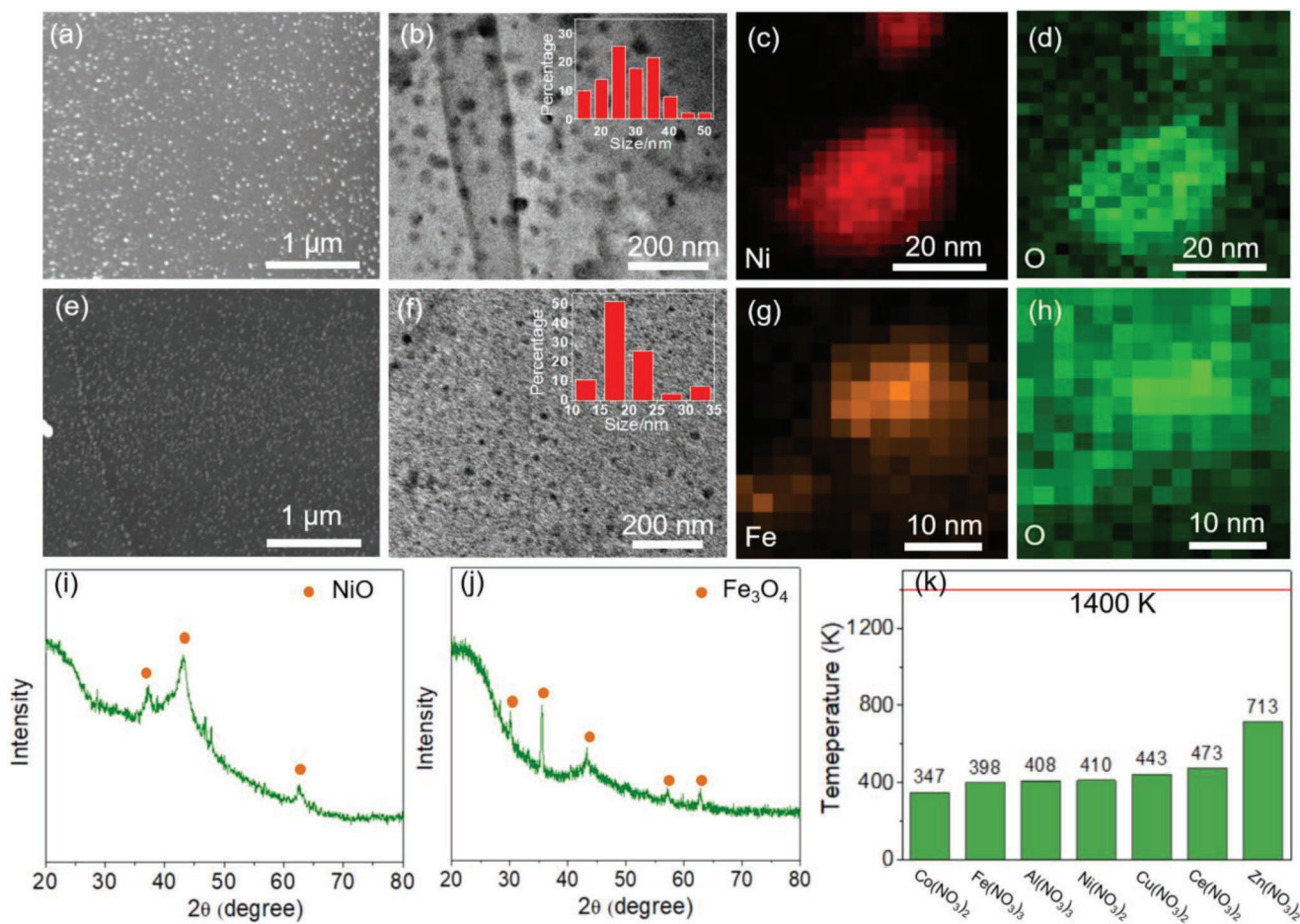


Figure 5. 3D heating as a universal metal oxide synthesis method. a) SEM, b) TEM, and c,d) elemental mapping of C-wood/NiO synthesized by 3D heating. e) SEM, f) TEM, and g,h) elemental mapping of C-wood/ Fe_3O_4 synthesized by 3D heating. XRD patterns of i) C-wood/NiO and j) C-wood/ Fe_3O_4 . k) Decomposition temperatures of selected metal nitrates in relation to the average 1400 K temperature of the reported 3D heating method.

with a maximum instantaneous ramping rate of $\approx 272\,000\text{ K s}^{-1}$, which is several orders of magnitude higher than that of conventional heating methods. The moderate conductivity, good thermal conductivity, and intact channeled structure of the C-wood substrate play important roles in the triggering of this 3D bulk heating effect due to the material's capability to absorb microwave energy. The high temperature contributes to the swift decomposition of precursor salts and recrystallization within a short time (4 s), leading to the formation of ultrafine metal oxide nanoparticles in C-wood. Besides CoO_x , we also successfully synthesized other metal oxide nanoparticles, including Fe_3O_4 and NiO , suggesting that the method can be extended to the synthesis of a wide range of metal oxide nanoparticles, so long as the precursor decomposition temperatures are lower than 1400 K. This rapid, universal, and bulk heating method based on microwaves represents a promising direction for the scalable synthesis of ultrafine metal oxide nanoparticles.

4. Experimental Section

Fabrication of the C-Wood/Nanoparticles: A piece of basswood (from Walnut Hollow Company) was calcined at 533 K for 6 h in air and at 973 K for 2 h in Ar to give the C-wood product. C-wood samples with different conductivities were obtained by adjusting the carbonization conditions (873 K/2 h, 1073 K/2 h, 1173 K/2 h, 1273 K/2 h). Metal nitrate precursors (>98%, Sigma-Aldrich) were dissolved in a 1:1 volume mixture of ethanol and deionized water at a concentration of 0.1 M. Then, a piece of C-wood (30 mm \times 15 mm \times 3 mm) was immersed into the precursor solution for 10 min, followed by drying at 333 K for 20 min. The C-wood/precursor was directly microwaved at 1000 W for various times in a domestic microwave oven.

Materials Characterization: The microstructure and morphology of the samples were characterized using a TESCAN VEGA-3-SBH SEM at 15 kV. TEM measurements were conducted using a JEOL JEM-2010 electron microscope equipped with an EDX spectrometer operating at an acceleration voltage of 200 kV.

Specifically, the as-prepared sample were ground in a mortar for 10 min, dispersed into ethanol and sonicated for 10 min, forming a $\approx 5\text{ mg mL}^{-1}$ suspension. 10 μL of the resulted suspension was dropped onto a copper grid and dried for TEM characterization. The XRD profiles were measured on D8 Advanced X-ray Diffraction system. Raman spectra were measured using a Horiba Jobin-Yvon instrument (Labram Aramis model) with laser wavelength of 532 nm and integration time of 4 s repeated for four scans.

Supporting Information

Supporting Information is available from the Wiley Online Library or from the author.

Acknowledgements

G.Z., S.X., and C.C. contributed equally to this work. L.H. acknowledges the financial support from the Dean's office of Department of Materials Science and Engineering for the equipment setup. The authors acknowledge the support of the Maryland NanoCenter and its AIMLab. G.Z. acknowledges the financial support of the China Scholarship Council. The authors acknowledge Dr. Xizheng Wang for the temperature measurement and Glenn Pastel for the Raman spectra measurement. L.H., G.Z., and S.X. designed the experiments. G.Z. contributed to the materials synthesis. C.C. contributed to the data analysis. M.R.Z.

and D.J.K. contributed to the temperature measurement. C.W. and M.G. contributed to the electromagnetic interference shielding characterization. G.Z., M.J., R.M., and H.X. contributed to the materials characterization. D.L. contributed to the 3D illustrations. L.H., G.Z., S.X., and C.C. contributed to the writing of the paper. All authors contributed to commenting on the final manuscript.

Conflict of Interest

The authors declare no conflict of interest.

Keywords

high temperature, in situ synthesis, instant heating, metal oxide nanoparticles, microwave

Received: May 28, 2019

Revised: August 3, 2019

Published online: September 19, 2019

- [1] N. L. Torad, M. Hu, S. Ishihara, H. Sukegawa, A. A. Belik, M. Imura, K. Ariga, Y. Sakka, Y. Yamauchi, *Small* **2014**, *10*, 2096.
- [2] Y. Yang, H. Chen, X. Zheng, X. Meng, T. Zhang, C. Hu, Y. Bai, S. Xiao, S. Yang, *Nano Energy* **2017**, *42*, 322.
- [3] F. Wang, D. Kozawa, Y. Miyauchi, K. Hiraoka, S. Mouri, Y. Ohno, K. Matsuda, *Nat. Commun.* **2015**, *6*, 6305.
- [4] X. Yu, T. J. Marks, A. Facchetti, *Nat. Mater.* **2016**, *15*, 386.
- [5] J. Yu, W. Lu, J. P. Smith, K. S. Booksh, L. Meng, Y. Huang, Q. Li, J. Byun, Y. Oh, Y. Yan, T.-W. Chou, *Adv. Energy Mater.* **2017**, *7*, 1600976.
- [6] M. F. El-Kady, Y. Shao, R. B. Kaner, *Nat. Rev. Mater.* **2016**, *1*, 16033.
- [7] C. Zhao, C. Yu, M. Zhang, H. Huang, S. Li, X. Han, Z. Liu, J. Yang, W. Xiao, J. Liang, X. Sun, J. Qiu, *Adv. Energy Mater.* **2017**, *7*, 1602880.
- [8] G. Huang, F. Zhang, X. Du, Y. Qin, D. Yin, L. Wang, *ACS Nano* **2015**, *9*, 1592.
- [9] M. Li, H. Du, L. Kuai, K. Huang, Y. Xia, B. Geng, *Angew. Chem., Int. Ed.* **2017**, *56*, 12649.
- [10] G. Mills, P. Mullinger, B. Jenkins, *Industrial and Process Furnaces Principles, Design and Operation*, Elsevier, Oxford, UK **2011**, p. 109.
- [11] Z. Qin, J. C. Bischof, *Chem. Soc. Rev.* **2012**, *41*, 1191.
- [12] J. Zhang, M. Ren, L. Wang, Y. Li, B. I. Yakobson, J. M. Tour, *Adv. Mater.* **2018**, *30*, 1707319.
- [13] L. Tao, H. Tian, Y. Liu, Z. Ju, Y. Pang, Y. Chen, D. Wang, X. Tian, J. Yan, N. Deng, Y. Yang, T. Ren, *Nat. Commun.* **2017**, *8*, 14579.
- [14] K. W. Tan, B. Jung, J. G. Werner, E. R. Rhoades, M. O. Thompson, U. Wiesner, *Science* **2015**, *349*, 54.
- [15] I. Bilecka, M. Niederberger, *Nanoscale* **2010**, *2*, 1358.
- [16] D. Voiry, J. Yang, J. Kupferberg, R. Fullon, C. Lee, H. Y. Jeong, H. S. Shin, M. Chhowalla, *Science* **2016**, *353*, 1413.
- [17] H. Fei, J. Dong, C. Wan, Z. Zhao, X. Xu, Z. Lin, Y. Wang, H. Liu, K. Zang, J. Luo, S. Zhao, W. Hu, W. Yan, I. Shakir, Y. Huang, X. Duan, *Adv. Mater.* **2018**, *30*, 1802146.
- [18] Y. Sun, L. Yang, K. Xia, H. Liu, D. Han, Y. Zhang, J. Zhang, *Adv. Mater.* **2018**, *30*, 1803189.
- [19] K. Paromita, C. Nethravathi, P. A. Deshpande, M. Rajamathi, G. Madras, N. Ravishankar, *Chem. Mater.* **2011**, *23*, 2772.
- [20] W. Zheng, P. Zhang, J. Chen, W. B. Tian, Y. M. Zhang, Z. M. Sun, *J. Mater. Chem. A* **2018**, *6*, 3543.
- [21] L. Hallopeau, D. Bregirou, G. Rousse, D. Portehault, P. Stevens, G. Toussaint, C. Laberty-Robert, *J. Power Sources* **2018**, *378*, 48.

- [22] R. Shmulsky, P. D. Jones, *Forest Products and Wood Science*, Wiley-Blackwell, Chichester, UK **2019**, p. 142.
- [23] C. Chen, Y. Zhang, Y. Li, J. Dai, J. Song, Y. Yao, Y. Gong, I. Kierzewski, J. Xie, L. Hu, *Energy Environ. Sci.* **2017**, *10*, 538.
- [24] L. Lu, Y. Lu, Z. Xiao, T. Zhang, F. Zhou, T. Ma, Y. Ni, H. Yao, Sh. Yu, Y. Cui, *Adv. Mater.* **2018**, *30*, 1706745.
- [25] J. Song, C. Chen, Z. Yang, Y. Kuang, T. Li, Y. Li, H. Huang, I. Kierzewski, B. Liu, S. He, T. Gao, S. U. Yuruker, A. Gong, B. Yang, L. Hu, *ACS Nano* **2018**, *12*, 140.
- [26] C. Chen, Y. Li, J. Song, Z. Yang, Y. Kuang, E. Hitz, C. Jia, A. Gong, F. Jiang, J. Y. Zhu, B. Yang, J. Xie, L. Hu, *Adv. Mater.* **2017**, *29*, 1701756.
- [27] M. Zhu, Y. Li, G. Chen, F. Jiang, Z. Yang, X. Luo, Y. Wang, S. D. Lacey, J. Dai, C. Wang, C. Jia, J. Wan, Y. Yao, A. Gong, B. Yang, Z. Yu, S. Das, L. Hu, *Adv. Mater.* **2017**, *29*, 1704107.
- [28] J. Song, C. Chen, S. Zhu, M. Zhu, J. Dai, U. Ray, Y. Li, Y. Kuang, Y. Li, N. Quispe, Y. Yao, A. Gong, U. H. Leiste, H. A. Bruck, J. Y. Zhu, A. Vellore, H. Li, M. L. Minus, Z. Jia, A. Martini, T. Li, L. Hu, *Nature* **2018**, *554*, 224.
- [29] R. Jacob, D. Kline, M. R. Zachariah, *J. Appl. Phys.* **2018**, *123*, 115902.
- [30] S. Xu, Y. Chen, Y. Li, A. Lu, Y. Yao, J. Dai, Y. Wang, B. Liu, S. D. Lacey, G. R. Pastel, Y. Kuang, V. A. Danner, F. Jiang, K. K. Fu, L. Hu, *Nano Lett.* **2017**, *17*, 5817.
- [31] Y. Yao, Z. Huang, P. Xie, S. D. Lacey, R. Jacob, H. Xie, F. Chen, A. Nie, T. Pu, M. Rehwoldt, D. Yu, M. R. Zachariah, C. Wang, R. Shahbazian-Yassar, J. Li, L. Hu, *Science* **2018**, *359*, 1489.
- [32] T. Kim, J. Lee, K. Lee, *Carbon Lett.* **2014**, *15*, 15.
- [33] K. MacKenzie, O. Dunens, A. T. Harris, *Sep. Purif. Technol.* **2009**, *66*, 209.
- [34] J. A. Menéndez, A. Arenillas, B. Fidalgo, Y. Fernández, L. Zubizarreta, E. G. Calvo, J. M. Bermúdez, *Fuel Process. Technol.* **2010**, *91*, 1.
- [35] R. Roy, D. Agrawal, J. Cheng, S. Gedevarshvili, *Nature* **1999**, *399*, 668.
- [36] H. Melikyana, T. Sargsyana, A. Babajanyana, S. Kima, J. Kim, K. Lee, B. Friedman, *J. Magn. Magn. Mater.* **2009**, *321*, 2483.
- [37] W. Xia, R. Zou, L. An, D. Xia, S. Guo, *Energy Environ. Sci.* **2015**, *8*, 568.
- [38] R. Meredith, *Engineer's Handbook of Industrial Microwave Heating*, The Institution of Electrical Engineers, London, UK **1988**, pp. 1–10.